

# Image demosaicing and reconstruction of bayer-patterned color images from color CCD samples using high-quality linear interpolation

Vishakha Goyal  
International Institute of Management, Engineering  
& Technology  
Jaipur  
Email:goyal.vishakha0@gmail.com

Nitin Khandelwal  
International Institute of Management, Engineering  
& Technology  
Jaipur  
Email:nitin.iimet@gmail.com

**Abstract** — A simplified color image formation model is used to construct an algorithm for image reconstruction from CCD sensors samples. The proposed method involves two successive steps. The first is motivated by Cok's template matching technique, while the second step uses steerable inverse diffusion in color. Classical linear signal processing techniques tend to over smooth the image and result in noticeable color artifacts along edges and sharp features. The question is how the different color channels should support each other to form the best possible reconstruction. Our answer is to let the edges support the color information and the color channels support the edges, and thereby achieve better perceptual results than those that are bounded by the sampling theoretical limit. This paper introduces a new interpolation technique for Demosaicing of color images produced by single-CCD digital cameras. We show that the proposed simple linear filter can lead to an improvement in PSNR when compared to a recently introduced linear interpolator. The proposed filter also outperforms most nonlinear demosaicing algorithms, without the artifacts due to nonlinear processing, and a much reduced computational complexity.

**Keywords**—Color enhancement, false color, image reconstruction, multichannel nonlinear image processing, steerable, Color filter array demosaicking, color interpolation, image measure, zipper effect.

## 1. INTRODUCTION

In recent years, digital cameras for still images and movies became popular. There are many obvious advantages to digital images comparing to classical film based cameras, yet there are limitations as well. For example, the spatial resolution is limited due to the physical structure of the sensors. "Super resolution" beyond the sensors resolution can be achieved by considering a sequence of images. For each  $2 \times 2$  set of pixels, two diagonally opposed pixels have green filters, and the other two have red and blue filters. Since G carries most of the luminance information, its sampling rate is twice that of R and B. We call demosaicing the

problem of interpolating back the image captured with a CFA, so that for every CCD pixel we can associate a full RGB value. The simplest approach to demosaicing is bilinear interpolation, in which the three color planes are independently interpolated using symmetric bilinear interpolation from the nearest neighbors of the same color. As expected, bilinear interpolation generates significant artifacts, especially across edges and other high-frequency content, since it doesn't take into account the correlation among the RGB values.

Practical demosaicing algorithms take such correlation into account either with better linear filters, or with nonlinear filters that adapt interpolation smoothness to a measure of image activity or edginess. In this work, we deal with the reconstruction of a single color digital image from its color CCD sensors' information. We limit our discussion to Bayer color filter array (CFA) pattern as presented in Fig. 1. We will start with a simple color image formation model and explore the relation between the different color channels such that the channels support the edges, and the edges support the colors. This relation with a simple color image formation model enables a reconstruction beyond the linear optimal signal processing approach that is limited by the Nyquist sampling rate. We follow Cok's exposition for constructing the first step of the algorithm: the reconstruction stage. The green component is reconstructed first with the help of the red and blue gradients. Then the red and blue are reconstructed using the green values, edge approximations, and a simple color ratio rule: Within a given "object" the ratio is locally constant the same is true for. This rule falls apart across edges where the color gradients are high, which are the interesting and problematic locations from our reconstruction point of view. We limit our discussion to further Flowchart of the interpolation step as presented in Fig. 2.

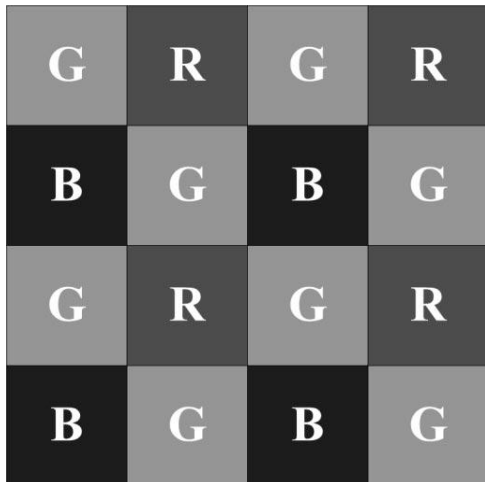


Figure 1. Schematic diagram of the Bayer color filter array pattern

Next, the green, red, and blue pixels are adjusted to fit the color cross ratio equivalence. The interpolation and the adjustment are weighted by a function of the directional derivatives to reduce the influence of ratios across edges. This is the main difference from Cok's method, who try to match templates that predict the local structure of the image for a bilinear interpolation. The second step, the enhancement stage, involves an anisotropic inverse diffusion flow in color space, which is an extension of Gabor's geometric filter, and is based on the geometric framework for color introduced. It is also related to Weickert's texture enhancement method, and to the recent results of Sapiro and Ringach, and Cottet and El Ayyadi. The idea is to consider the color image as a two-dimensional (2-D) surface in five-dimensional (5D)

$(x,y,R,G,B)$  space, extract its induced metric and smooth the metric in order to sense the structure of the image surface beyond the local noise. Then diffuse the different channels along the edges and simultaneously enhance the image by applying an "inverse heat" operator across the edges. The structure of this paper is as follows. Section II introduces a simple model for color images. Section III introduces a simple model of Interpolation Step. Next Section IV uses this model for the reconstruction of a one-dimensional (1-D) image. Section V presents the first step of the algorithm, the reconstruction stage that involves weighted interpolation subject to constant cross ratio of the spectral channels. Section VI presents the second step of the algorithm. It is a nonlinear enhancement filter based on steerable anisotropic inverse diffusion flow in color space. Section VI concludes with experimental results on a set of benchmark images. In this paper we present a simple linear demosaicing filter, with better performance and lower complexity than that in [4]. Our filter also outperforms many nonlinear algorithms. In Section II we quickly review some of the techniques proposed for improved demosaicing

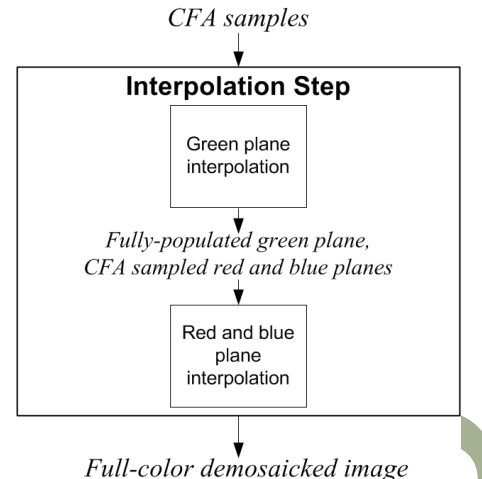


Figure 2. Flowchart of the interpolation step.

performance, Section III overview of interpolation step and in Section IV we present our new 1-D image and Section V reconstruction of linear filter. Enhancement and Post processing Step in Section VI and VII. Image measures for demosaicing performance in Section VIII. Experimental result and conclusions are presented in Sections IX and X respectively.

## II. SIMPLE COLOR IMAGE FORMATION

A simplified model for color images is a result of viewing Lambertian non flat surface patches. Such a scene is a generalization of what is known as a "Mondriaan world." According to the model, each channel may be considered as the projection of the real three-dimensional (3-D) world surface normal on to the light source direction, multiplied by the albedo. The albedo captures the characteristics of the 3-Object's material, and is different for each of the spectral channels. That is, the three color channels may be written as

$$I^R(x) = \rho R(x) \langle \hat{N}(x), \bar{l} \rangle \quad (1)$$

$$I^G(x) = \rho G(x) \langle \hat{N}(x), \bar{l} \rangle \quad (2)$$

$$I^B(x) = \rho B(x) \langle \hat{N}(x), \bar{l} \rangle \quad (3)$$

This means that the different colors capture the change in material via  $\rho_i$  (where  $i$  stand for R, G, and B) that multiplies the normalized shading image  $\bar{I}(x) = \langle \hat{N}(x), \bar{l} \rangle$ . The Mondriaan color image formation model was used for color based segmentation and shading extraction from color images. Let us follow the above generalization of this model and assume that the materials, and therefore the albedo, are the same within a given object in the image, e.g.  $\rho_i(x) = C_i$ , where  $C_i$  is a given constant. Thus, within the interior of a given object the following constant ratio holds:

$$\frac{I_i(x)}{I_j(x)} = \frac{\rho_i(x)}{\rho_j(x)} = \frac{C_i}{C_j} \quad (4)$$

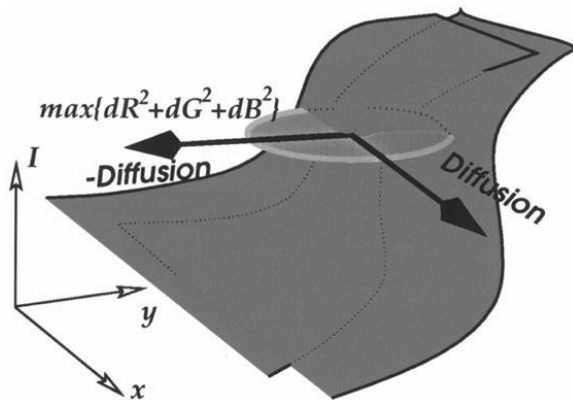


Figure 3. Red and green components painted as surfaces in with the inverse diffusion (across the edge) and diffusion (along the edge) directions.

That is, the color ratio within a given object is constant. We note that this is an oversimplified assumption for general analysis of color images. However, its local nature it makes valid and useful for our technological purpose. That is, the color ratio within a given object is constant.

### III. INTERPOLATION STEP

We describe in this section the first step of our proposed demosaicking method, an interpolation step that progressively renders a full-color image from CFA samples the flowchart of this interpolation step; the green plane is the first to be interpolated and, once fully populated, used to assist the subsequent red and blue plane interpolation. Although processed in a sequential order, the three color planes are interpolated in the same manner. Specifically, every missing color value is interpolated by properly combining the estimates obtained from its four interpolation directions, which are defined according to the four nearest CFA samples of the same color. The estimate from one particular interpolation direction is obtained by exploiting the spectral correlation among the neighboring pixels along that direction. The spectral correlation refers to the assumption that the differences between the green and red/blue values within a local neighborhood are well correlated with constant offsets. However, this spectral correlation is defined for the color values at each individual pixel, which are not fully available from the CFA samples. To make use of this spectral correlation, we further assume that the rate of change of neighboring pixel values along an interpolation direction also a constant.

|                  |                 |                 |                 |                 |                 |                 |
|------------------|-----------------|-----------------|-----------------|-----------------|-----------------|-----------------|
| R <sub>11</sub>  | G <sub>12</sub> | R <sub>13</sub> | G <sub>14</sub> | R <sub>15</sub> | G <sub>16</sub> | R <sub>17</sub> |
| Top direction    |                 |                 |                 |                 |                 |                 |
| G <sub>21</sub>  | B <sub>22</sub> | G <sub>23</sub> | B <sub>24</sub> | G <sub>25</sub> | B <sub>26</sub> | G <sub>27</sub> |
| R <sub>31</sub>  | G <sub>32</sub> | R <sub>33</sub> | G <sub>34</sub> | R <sub>35</sub> | G <sub>36</sub> | R <sub>37</sub> |
| Left direction   |                 |                 |                 |                 |                 |                 |
| G <sub>41</sub>  | B <sub>42</sub> | G <sub>43</sub> | B <sub>44</sub> | G <sub>45</sub> | B <sub>46</sub> | G <sub>47</sub> |
| R <sub>51</sub>  | G <sub>52</sub> | R <sub>53</sub> | G <sub>54</sub> | R <sub>55</sub> | G <sub>56</sub> | R <sub>57</sub> |
| Right direction  |                 |                 |                 |                 |                 |                 |
| G <sub>61</sub>  | B <sub>62</sub> | G <sub>63</sub> | B <sub>64</sub> | G <sub>65</sub> | B <sub>66</sub> | G <sub>67</sub> |
| Bottom direction |                 |                 |                 |                 |                 |                 |
| R <sub>71</sub>  | G <sub>72</sub> | R <sub>73</sub> | G <sub>74</sub> | R <sub>75</sub> | G <sub>76</sub> | R <sub>77</sub> |

Figure 4. A 7\_7 window where the green value of the central pixel is to be estimated.

Clearly, all these assumptions fail to hold in the presence of sharp edges and fine details, where color values experience abrupt changes. The abrupt changes of color values indicate low spatial correlation among neighboring pixels. Intuitively, the higher the spatial correlation among pixels along an interpolation direction, the more accurate the estimate of a missing color value can be obtained from that direction. Therefore, to interpolate one missing color value, we combine the estimates from its four interpolation directions by assigning them with weights that measure the spatial correlations among the neighboring pixels along the corresponding interpolation directions. Note that although the missing color values at each pixel will be progressively interpolated, we shall denote pixels as red, green and blue pixels according to the color of their original CFA samples.

### IV. THE 1-D CASE

Let us start with a simple 1-D example with two colors; see Fig. 2. Our assumption is that the colors are smooth within a given object and go through a sudden jump at the boundaries. Define the central difference approximation to be  $D_x I_i = \frac{(I_{i+1} - I_{i-1}))}{\Delta x}$ , where  $I_i = I(\Delta x)$  is the value of the function  $I(x)$  at the point  $x=i \Delta x$  and  $\Delta x$  is the spatial discretization interval.

Given the samples (odd points for the red and even points for the green) we use the gradient to construct an edge indicator for the interpolation. Let the edge indicator be  $e_g^i = f(D_x G_i)$  where  $f(0)$  is a decreasing function, e.g.,  $e_g^i = 1 + (D_x G_i)2) - 0.5$ , and,  $e_r^i$  respectively. One simple reconstruction procedure is as follows.

- Init: Interpolate for the green at the missing points

$$G_i = \frac{e_{i-1}^r G_{i-1} + e_{i-1}^g G_{i+1}}{e_{i-1}^r + e_{i-1}^g} \tag{5}$$

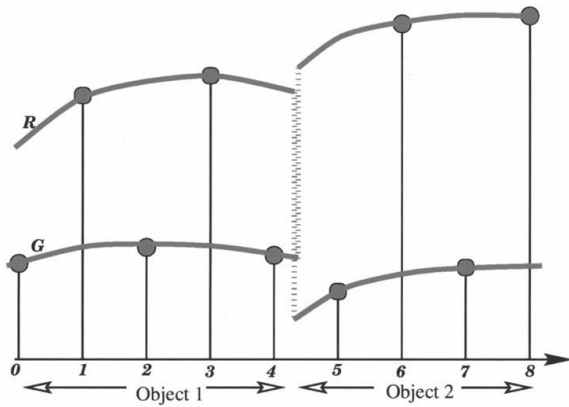


Figure 5. Red and green components of a 1-D image.

- Repeat for three times:
- Interpolate the red values via the ratio rule weighted by the edge indicator

$$R_i = G_i \frac{e_{i-1}^g \frac{R_{i-1} + e_{i-1}^g R_{i+1}}{e_{i-1}^g + e_{i+1}^g}}{e_{i-1}^g + e_{i+1}^g}$$

(6)

- Correct the green values to fit the ratio rule

$$R_i = G_i \frac{e_{i-1}^r \frac{G_{i-1} + e_{i-1}^r G_{i+1}}{e_{i-1}^r + e_{i+1}^r}}{e_{i-1}^r + e_{i+1}^r}$$

(7)

- End of loop.

Note that this is a numerically consistent procedure for the proposed color image formation model. It means that as the sampling grid is refined, the result converges to the continuous solution. Here again we recognize the importance of segmentation in computer vision. An accurate segmentation procedure, that gives the exact locations of the objects boundaries, would have allowed an image reconstruction far beyond the sampling limit (under the assumption that within a given object there are no high spatial frequencies).

#### V. FIRST STEP: RECONSTRUCTION

For real 2-D images with three color channels the reconstruction is less trivial. Edges now become curves rather than points, and in many cases one needs to interpolate missing points along the edges. We would still like to avoid interpolating across edges. Based on the simplified color image formation model, the three channels go through a sudden jump across the edges.

Thus, the gradient magnitude can be used as an edge indicator, and its direction can approximate the edge direction [it is easy to verify that the gradient of  $G$  is normal to the level set curves of  $G(x)$ , i.e.  $G(x) = \text{constant}$ . The directional derivatives are approximated at each point based on its eight nearest neighbors on the grid. Define the finite difference approximation for the directional derivatives, central  $D$ , forward  $D+$ , and backward  $D-$ . At the green points use  $\max\{D_x^+ G_{i,j}, D_x^- G_{i,j}\}$  for the magnitude of the directional

derivative along the direction for the rest of the points and the directions use central differences. We thereby construct an approximation for the directional derivatives at each and every point.

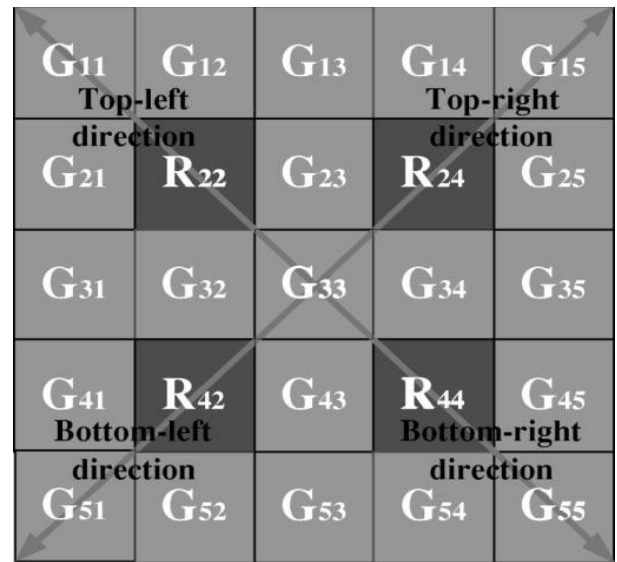


Figure 6. A 5\_5 window where the red value of the central pixel is to be estimated.

- Next, we generalize an edge indicator function. When a point  $\{(i + 1) \Delta x, j \Delta y\}$  at location is taking part in the interpolation  $(i \Delta x, j \Delta y)$  at the location, we use the following weight as an edge indicator. Based on the edge indicators as weights for the interpolation we follow similar steps as for the 1-D case to reconstruct the 2-D image.

Init: Interpolate for the green at the missing points as in, shown at the figure 3. Interpolate for the blue and red in Steps 6 and 7.

- Repeat for three times:
- Correct the green values to fit the ratio rule and average between the blue and red interpolation results

$$G_{i,j} = \frac{G_{i,j}^B + G_{i,j}^R}{2}$$

- Correct the blue and red values via the ratio rule weighted by the edge indicator up to this point, the original values given as samples were not modified. We have interpolated the missing points weighted by edge indicator functions subject to the constant cross ratio. Next, we apply inverse diffusion in color to the whole image as an enhancement filter.

#### VI. SECOND STEP: ENHANCEMENT

This section is a brief description of one of the nonlinear filters introduced in [7] that we apply as a second step for enhancing the color image. In [6], Gabor considered an image enhancement procedure based on an anisotropic flow via the inverse second directional derivative in the “edge” direction and the geometric heat equation as diffusion along the edge, see also [5]. Cottet and Germain [3] used a smoothed version of the image to direct the diffusion. Weickert smoothed the “structure

tensor” and then manipulated its Eigen values to steer the smoothing direction, while Sapiro and Ringach eliminated one Eigen value from the structure tensor in color space without smoothing its coefficients. Motivated by all of these results, a new color enhancement filter was introduced in [8]. The inverse diffusion and diffusion directions are deduced from the smoothed metric coefficients of the image surface. The color image is considered as a 2-D surface in the 5-D space  $(x, y, R, G, B)$ , as suggested in [8]. The induced metric coefficients are extracted for the image surface and used as a natural structure tensor for the color case.

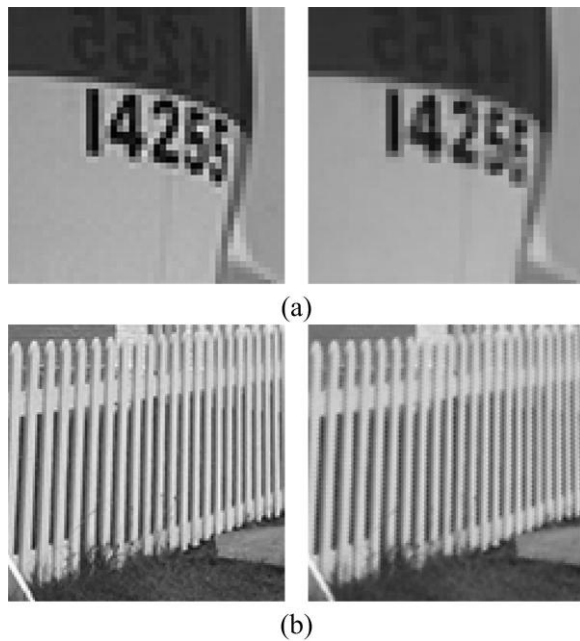


Figure 7. (a) Example of false colors and (b) example of zipper effect.

The induced metric is a symmetric matrix that captures the geometry of the image surface. Let  $A_1$  and  $A_2$  be the largest and the smallest Eigen values  $u_1$  and  $u_2$  of, respectively. Since  $M$  is a symmetric positive matrix it's corresponding. Let us use the image metric as a structure tensor. We extract the structure from the metric and then modify it to be a nonsingular symmetric matrix with one positive and one negative Eigen values. That is, instead of diffusion we introduce an inverse diffusion in the edge direction (across the edge). This is an extension of Gabor's idea [6] of inverting the diffusion along the gradient direction. The proposed inverse diffusion enhancement for color images is then given as follows.

- 1) Compute the metric coefficients  $g_{u,v}$  or explicitly after that in equation.
- 2) Diffuse the coefficients  $g_{u,v}$  by convolving with a Gaussian of variance  $\rho$ .
- 3) Change the Eigen values  $g_{u,v}$  of such that the largest

Eigen value is  $A_1$  now and, for some given positive scalar  $\lambda$ . This yields a new matrix. A single scalar is chosen for simplicity of the presentation. Different eigenvalues can be chosen, like Eigen values  $A_1$  and  $A_2$  that depend on the original ones. The important idea is to set the original largest Eigen value to a negative value.

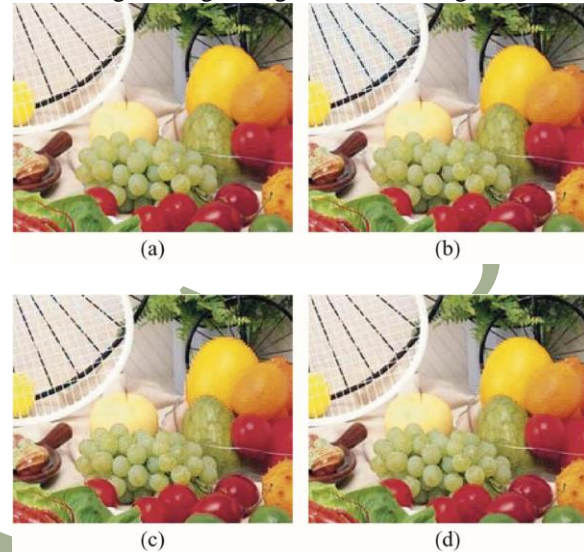


Figure 8. (a) Nonmosaicked original from Bike image and demosaicked results obtained from (b) Li's method, (c) Gunturk's method, and (d) the proposed method

This operation inverts the diffusion direction across the color edge and thereby enhance it CCD image.

- 4) Evolve the channel via the flow channel  $k$ . Inverting the heat equation is an inherently unstable process. However, if we keep smoothing the metric coefficients, and apply the diffusion along the edge (given the positive Eigen value),

We get a coherence-enhancing flow that yields sharper edges and is stable for a short duration of time.

#### VII. POST-PROCESSING STEP

The proposed post-processing step aims to suppress visible artifacts residing in the initial demosaicked images obtained from the aforementioned interpolation step. There are two main types of demosaicking artifacts, namely false colors and zipper effect. False colors are those artifacts corresponding to noticeable color errors as compared to the original, nonmosaicked image. One example is shown in Fig. 7(a), where the left hand is a full-color image and the right hand is its demosaicked image with false colors around the numbers region. The zipper effect refers to abrupt or unnatural changes of color differences between neighboring pixels, manifesting as an “on-off” pattern. One example is shown in Fig. 7(b), where the left hand is a full-color image and the right hand is its demosaicked image with the zipper effect around the fence region.

As demosaicking artifacts often exhibit as color outliers, Freeman [3] proposed to use a median filter to process the inter-channel differences (red-green and blue-green) of demosaicked images obtained by bilinear interpolation. The rationale is that median filtering the inter-channel difference can force pixels with distinct colors to be more similar to their neighbors, thus eliminating color outliers or errors. Note that in Freeman's method, the original CFA-sampled color value at each pixel is not altered, and it is combined with median-filtered inter-channel differences to obtain the other two missing color values. In general, Freeman's method is rather effective in suppressing demosaicking artifacts, while preserving sharp edges. However, when applying this method to post-process the initial demosaicked images obtained from our proposed interpolation step, we observed that some demosaicking artifacts still remain around sharp edges and fine details. This is partly due to the fact that each pixel has two independent inter-channels differences, and filtering the differences separately does not take into account the spectral correlation between color planes. To make use of the spectral correlation, one intuitive extension of Freeman's method is to adopt a vector median filter which takes as input the vector of two inter-channel differences.

However, we found this extension barely shows any improvement in suppressing artifacts as compared to Freeman's method. This is because when the three color planes are separately interpolated, the estimation errors incurred in different color planes, which can be regarded as additive noise, are rather independent from each other. It has been shown in [8] that when the noise is independent in different vector components, the vector-based median filtering cannot outperform the component-wise median filtering in suppressing noise. To incorporate median filtering with the spectral correlation for more effective suppression of demosaicking artifacts, we lift the constraint of keeping the original CFA-sampled color values intact. Furthermore, we make use of the latest processed color values to filter the subsequent pixels so that estimation errors can be effectively diffused into local neighborhoods. Specifically, we adjust the three color values at the central pixel of a local window (the window size is equal to the support of the median filter). Experimental results show that this post-processing step is capable of suppressing most visually annoying artifacts. The first column of Fig. 8 shows the originals of two test image regions: the trousers region in Barbara image and the fence region in Lighthouse image. (Fig. 8) The fine details in these two regions pose great challenges to many demosaicking methods. The second column of Fig. 8 shows the initial demosaicked images, which have some visible false colors and zipper artifacts, obtained by the proposed interpolation step. We

then post-process them with Freeman's method and our post-processing step; the results are shown in the third and fourth columns of Fig. 8, respectively. It is clear that our proposed post-processing step can perform noticeably better than Freeman's method. Although effective in eliminating most demosaicking artifacts, the proposed post-processing method, like many other median filtering schemes, may de-saturate the color of demosaicked images if applied indiscriminately. To strike a good balance between suppression of demosaicking artifacts and preservation of color fidelity, the post-processing step is only selectively applied around image regions that are prone to demosaicking artifacts. We detect these artifact-prone regions as follows.

#### VIII. IMAGE MEASURES FOR DEMOSAICKING PERFORMANCE

While a large number of demosaicking methods have been proposed in the literature, there is, however, a lack of image measures which can effectively quantify the performance of these methods. Ideally, from a psychological standpoint, effective image measures should be in accordance with perceptual judgments made by human observers. Such image measures could help simplify the development, improvement, and evaluation of different demosaicking methods, as they would rely much less on subjective test of image preference, which is not only time consuming but also dependent on the experimental settings and the subjects involved. It is generally agreed that current image measures cannot effectively quantify the perceptual quality of images obtained from a restoration process.

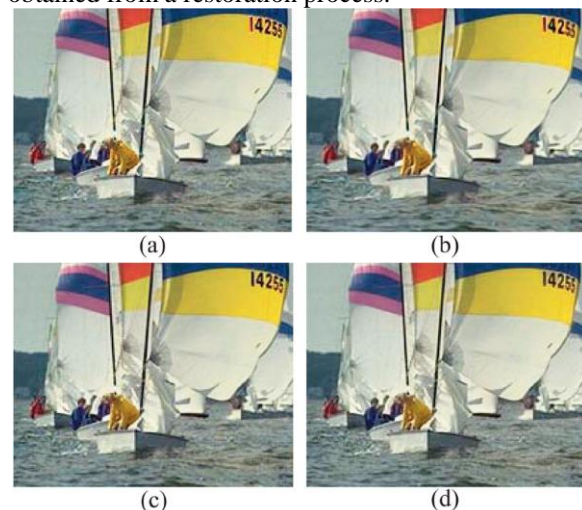


Figure 9. Demosaicked Small Sails image of (a) the first step and (b) the second step of Kimmel's method, as well as that of (c) the interpolation step and (d) the Post-processing step of our proposed method.

This limitation holds for CFA demosaicking and is supported by the recent experiments conducted by

Philippe et al on the subjective preference LU AND TAN: COLOR FILTER ARRAY DEMOSAICKING 1201. Their experiments reveal that when evaluated using the current image measures, some demosaicked results that are very different from the nonmosaicked originals are the most preferred. They also discover that many most-preferred results are sharpened by the demosaicking method under examination. Only when the image sharpness is removed as a salient factor, the nonmosaicked originals are the most preferred. As it remains unclear what factors are conducive to visually-pleasing images, we will treat demosaicking as a reconstruction process. In our view, since subjective image preference could vary from individual to individual, the images should be first reproduced as accurately as possible before any enhancement process, such as image sharpening, is applied. Therefore, we propose to quantify the performance of a demosaicking method from two aspects:

- 1) To measure the image fidelity of its demosaicked results as compared to the nonmosaicked originals and
- 2) To measure the amount of artifacts residing in the demosaicked results, in particular, the zipper effect.

#### IX. EXPERIMENTAL RESULTS

We tested the proposed method on four benchmark images that were sampled with Bayer color filter array pattern. The following examples demonstrate the reconstruction and enhancement results for four benchmark images statue, sails, window, and lighthouse. For each case, the top left is the original image. As a reference, we present the result of a bilinear interpolation for the missing points for each channel separately at the top right of each figure. The bottom left is the result of the first reconstruction by weighted interpolation step, and the bottom right is the second step enhancement result. View all images in color. The same parameters were used for the reconstruction in all the examples, i.e., case dependent tuning was not used for the different images.

#### X. CONCLUSION

In this paper, we have presented a new CFA demosaicking method that consists of two successive steps: an interpolation step that fills in missing color values in a progressive fashion by exploiting the spectral and spatial correlations among neighboring pixels, and a post-processing step that incorporates spectral correlation with median filtering of inter-channel differences to suppress demosaicking artifacts. To preserve the color fidelity of demosaicked images, the post-processing step is selectively applied to artifact-prone regions identified by a discrete Laplacian operator. When applied to the CFA samples of a variety of test images, the proposed method is able to generate demosaicked images with better perceptual

quality compared to that produced by other existing methods.

Several image measures are also proposed to quantify the performance of different demosaicking methods. Considering CFA demosaicking as a reconstruction process, we make use of original, nonmosaicked images as baselines to compare the results of different demosaicked methods. For each test image, we compute the PSNR and CIELAB values for the edge and smooth regions, separately. A new objective measure has also been devised to explicitly account for the zipper effect in demosaicked images. Experimental results show that the proposed image measures can effectively quantify the performance of different demosaicking methods.

#### REFERENCES

- [1] D. R. Cok, "Reconstruction of CCD images using template matching," in Proc. IS&T Ann. Conf./ICPS, 1994, pp. 380–385.
- [2] G. H. Cottet and M. El Ayyadi, "A Volterra type model for image processing," IEEE Trans. Image Processing, vol. 7, pp. 292–303, March 1998.
- [3] G. H. Cottet and L. Germain, "Image processing through reaction combined with nonlinear diffusion," Math. Comput. vol. 61, pp. 659–673, 1993.
- [4] P. T. Eliason, L. A. Soderblom and P. S. Chavez, "Extraction of topographic and spectral albedo information from multi spectral images," Photogram. Eng. Remote Sensing, vol. 48, pp. 1571–1579, 1981.
- [5] B. V. Funt, M. S. Drew, and M. Brockington, "Recovering shading from color images," in Lecture Notes in Computer Science: Computer Vision, ECCV'92, vol. 588 G. Sandini, Ed. Berlin, Germany: Springer-Verlag, 1992, pp. 124–132.
- [6] D. Gabor, "Information theory in electron microscopy," Lab. Investigat., vol. 14, pp. 801–807, 1965.
- [7] G. Healey, "Using color for geometry-insensitive segmentation," J. Opt. Soc. Amer. A, vol. 6, pp. 920–937, 1989.
- [8] R. Kimmel, R. Malladi, and N. Sochen, "Image processing via the beltrami operator," in Proc. 3rd Asian Conf. Computer Vision, Hong Kong, Jan. 1998.
- [9] M. Lindenbaum, M. Fischer, and A. M. Bruckstein, "On Gabor's contribution to image enhancement," Pattern Recognit., vol. 27, pp. 1–8, 1994.
- [10] G. Sapiro and D. L. Ringach, "Anisotropic diffusion of multivalued images with applications to color filtering," IEEE Trans. Image Processing, vol. 5, pp. 1582–1586, 1996.
- [11] N. Sochen, R. Kimmel, and R. Malladi, "A general framework for low level vision," IEEE Trans. Image Processing, vol. 7, pp. 310–318, 1998.
- [12] J. Weickert, "Anisotropic diffusion in image processing," PhD D. Cok, "Signal Processing Method and Apparatus for Producing Interpolated Chrominance

Values in a Sampled Color Image Signal,” U.S. patent 4 642 678, 1987.

[13] J. Adams, “Interactions between color plane interpolation and other image processing functions in electronic photography,” Proc. SPIE, vol. 2416, pp. 144–151, 1995.

[14] T. W. Freeman, “Median Filter for Reconstructing Missing Color Samples,” U.S. Patent 4 724 395, 1988.

[15] J. Weldy, “Optimized design for a single-sensor color electronic camera system,” Proc. SPIE, vol. 1071, pp. 300–307, 1990.

[16] H. Hibbard, “Apparatus and Method for Adaptively Interpolating a Full Color Image Utilizing Luminance Gradients,” U.S. Patent 5 382 976, 1996.

[17] C. Laroche and M. Prescott, “Apparatus and Method for Adaptively Interpolating a Full Color Image Utilizing Chrominance Gradients,” U.S. Patent 5 373 322, 1994.

[18] J. Hamilton and J. Adams, “Adaptive Color Plane Interpolation in Single Sensor Color Electronic Camera,” U.S. Patent 5 629 734, 1997.

[19] J. Adams, “Design of practical color filter array interpolation algorithms for digital cameras,” Proc. SPIE, vol. 3028, pp. 117–125, Feb. 1997.

[20] D. Cok, “Signal Processing Method and Apparatus for Sampled Image Signals,” U.S. Patent 4 630 307, 1986.

1, pp. 123–132, 2002.

[21] “Recommendations on Uniform Color Spaces, Color Difference Equations, Psychometric Color Terms,” C. I. E, Supplement no. 2 to CIE publication no. 15(E.-1 31) 1971/(TC-1.3), 1978.

[22] M. D. Fairchild, Color Appearance Models. Reading, MA: Addison Wesley, 1997.

[23] M. Mahy, E. Van, and O. A., “Evaluation of uniform color spaces developed after the adoption of CIELAB and CIELUV,” Color Res. Applicat., vol. 19, no. 2, pp. 105–121, 1994.

[24] A. Jain, Fundamentals of Digital Image Processing. Englewood Cliffs, NJ: Prentice-Hall, 1989.

[25] E. Wesley, L. Griff, and S. William, “Demosaicking methods for Bayer color arrays,” J. Electron. Image 2002.

[26] [Online] Available: <http://www.cs.technion.ac.il/~ron/Demosaic/>.